Fermi National Accelerator Laboratory

FERMILAB-Pub-81/16-EXP
7420.180
(Submitted to Phys. Lett. B)

CHARGE COMPENSATION IN THE QUARK JETS

Risto Orava

January 1981

Operated by Universities Research Association Inc. under contract with the Energy Research and Development Administration

Charge Compensation in the Quark Jets

Risto Orava*
Fermi National Accelerator Laboratory
P.O. Box 500, Batavia, IL 60510

Abstract

We sum cumulatively charges of hadrons produced over the range of rapidities in antineutrino-nucleon charged current interactions and show that the hypothesis of local charge conservation (LCC) is approximately valid above center-of-mass energies of 4 GeV. Charge compensation in the current fragmentation region seems to occur in a shorter rapidity interval than in proton-proton interactions at comparable centre-of-mass energies.

*On leave from the University of Helsinki, Helsinki, Finland.

1. Introduction

A sensitive test of a particular model for quark fragmentation into the observed hadron states is provided by the rapidity zone analysis.[1-3] By studying the charge variation as a function of rapidity one is able to verify how charge is compensated locally in rapidity space and learn about charge transfer along the rapidity axis. Information on the charge transfer between the current and target fragmentation regions is of special interest. Charge density has been studied earlier in Ref. 4.

The purpose of this study is to measure the variation of the summed or cumulative charge along the rapidity axis in antineutrino-nucleon charged current interactions. This is the first cumulative charge measurement in lepton produced hadronic final states and should prove useful in testing recent models of quark fragmentation.

For each individual event the tracks are ordered with increasing c.m.s. rapidity, $y^* = \frac{1}{2} \ln \left[(E^* + p^*_{\parallel}) / (E^* - p^*_{\parallel}) \right]$, where E^* is the hadron c.m. energy and $p^*_{\parallel}$ the hadron momentum component along the current direction. The cumulative charge $\sum_i e_i$, summed over hadrons with rapidity below that of the i^{th} final state particle, equals the charge transfer through y_i^*.

For illustration we show in Fig. 1 the zones, or regions where the cumulative charge $\Sigma_i e_i \neq 0$, and the gaps, i.e the regions separating the zones, with $\Sigma_i e_i = 0$. The function plotted in Fig. 1 is the zone graph

$$Z(y^*) = \sum_i e_i \theta(y^* - y_i^*) \qquad (1)$$

where $\theta(y^* - y_i^*)$ is the step function equal to 0 for negative arguments and equal to 1 elsewhere and the summation is extended over all charged hadrons in the final state. Each zone is defined by the following three parameters:

(1) n_Z, the number of tracks in zone Z

(2) y_Z. the average rapidity of zone Z; i.e., half sum of the rapidities of the first and last particle in the zone, and

(3) λ_Z, the distance between the rapidities defining a zone.

The hypothesis of local charge conservation (LCC) states that n_Z and λ_Z should become independent of W at sufficiently high energies.[1] In the following we shall test the LCC hypothesis in the antineutrino charged current induced quark jets.

2. The experiment

The experimental data come from exposure of the Fermilab 15-foot bubble chamber to a wide-band horn-focussed antineutrino beam and, in a second run, to a bare target sign selected antineutrino beam. The muons in the sample of charged current events are identified by the External Muon

Identifier (EMI) supplemented by a large transverse momentum procedure (BIGPT) described elsewhere.[6] The overall μ^+ identification efficiency is 92%, independent of muon production angle for muons with laboratory momenta larger than 4 GeV/c. The antineutrino energy spectrum peaks at 18 GeV and extends up to 200 GeV.

On the average 17% of the hadronic energy escapes detection in the bubble chamber. This analysis is performed using several energy reconstruction procedures, for example, event-by-event methods [7,8] and an average energy correction method.[9] The physics results presented here were found to be insensitive to the method employed and are actually based on the method of Ref. 8.

The antineutrino charged current event sample was required to have (a) a positively charged muon with momentum greater than 4 GeV/c and (b) a total momentum along the anti-neutrino direction larger than 7.5 GeV/c. The event sample passing these selection criteria consists of 7200 unweighted events.

Further details concerning the data sample used for this analysis can be found in Ref. 6.

3. Results

In the following we only consider charged final state hadrons travelling forward in the current direction in the $\bar{\nu}_\mu N$ charged current interactions; i.e, we require that the c.m. rapidity y^* is positive for each final state particle. We have shown earlier in Ref. 6 that this is a natural definition

of the "current fragmentation region". At low c.m. energies ($W \leq 4$ GeV/c) there is a significant overlap between the target ($y^* < 0$) and current fragmentation regions that one has to keep in mind when interpreting the results. To exclude quasi-elastic channels we require further that the lepton four-momentum transfer, $-q^2$, fulfills the condition $-q^2 > 1$ GeV^2/c^2.

Among the positively charged particles in the current fragmentation region ($y^* > 0$) there is a (15±3)% contribution from unidentified protons which have been assigned the pion mass.[10] These unidentified protons get shifted, on the average, about 0.7 units higher in rapidity due to the wrong mass assignment. We have studied effects of the unidentified protons in our analysis by utilizing the observed lambda-hyperons in our data sample and find the correction to the rapidity zone distributions to be negligible.

To observe possible effects due to the overlap between the current and target fragentation regions we shall use two alternative definitions for the rapidity zones in the forward centre-of-mass hemisphere (shaded regions in Fig. 1). We first define the rapidity zones in the current fragmentation region for particles strictly forward in the hadronic centre-of-mass system ($y^* > 0$; FORWARD ZONES I). Secondly, we allow for an overlap between the target fragmentation region as indicated in Fig. 1b (FORWARD ZONES II).

In Fig. 2 we show the average number of rapidity zones $\langle N_Z \rangle = \langle n_{ch} \rangle / \langle n_Z \rangle$ as a function of the average charged particle multiplicity $\langle n_{ch} \rangle$ for the two definitions (I and II), respectively. In Fig. 3 the length distribution of the rapidity zones, $dN_Z/d\lambda_Z \propto \exp(-\lambda_Z/\lambda_o)$, can be seen to be characteristic of models satisfying the short range correlation hypothesis (SRO). The rapidity zones in the current fragmentation region (solid circles in Fig. 3, FORWARD ZONES I) are seen to be significantly shorter, on the average, than the zones which include an overlapping zone with the target fragmentation region (solid squares in Fig. 3; FORWARD ZONES II). The average zone length is for the strictly forward rapidity zones $\langle \lambda_o \rangle = 0.57 \pm 0.01$ and for the zones which include an overlapping zone with the target fragmentation region (FORWARD ZONES II), $\langle \lambda_o \rangle = 0.95 \pm 0.01$.

We test the LCC hypothesis in Fig. 4 where the average zone length, $\langle \lambda_o \rangle$, and the average charged particle multiplicity in a zone, $\langle n_Z \rangle$, are plotted as functions of the c.m. energy W. For comparison, data from two proton-proton experiments[2,3] are also shown. At low c.m. energies ($W \leq 4$ GeV) a clear increase of $\langle \lambda_o \rangle$ and $\langle n_Z \rangle$ with W is observed. At c.m. energies of W>4 GeV, however, only weak dependence on W remains. The data points for central rapidity zones (obtained by excluding the target and beam fragments) in proton-proton experiments (open circles in Fig. 4) lie at slightly higher c.m. energies and roughly agree with our measurements for the rapidity zones in the current fragmentation region (FORWARD ZONES I), but strongly disagree with the zones which include an overlapping rapidity zone FORWARD ZONES II).

The average charged particle multiplicity in a zone, $\langle n_Z \rangle$, seems to be larger in the proton-proton induced central zones than in our rapidity zones in the current fragmentation region (Fig. 4b). If we include the overlapping zones, the multiplicities $\langle n_Z \rangle$ measured in this experiment are seen to be comparable to the results obtained in the pp-experiments (Fig. 4b).

As expected from kinematics we observe a logarithmic increase of the average zone rapidity $\langle y_Z \rangle$ as a function of W (Fig. 5).

4. Conclusions

We have analyzed rapidity zones in the hadronic final states of charged current antineutrino-nucleon interactions. The average length in rapidity required for hadron charge compensation is measured as an average zone length, $\langle \lambda_o \rangle$, and found to be in these lepton produced jets equal to 0.57 ± 0.01 units of rapidity. If an overlap with the target fragments is allowed in defining the rapidity zones a significantly longer average zone length is measured: $\langle \lambda_o \rangle = 0.95 \pm 0.01$. This result demonstrates the importance of the overlap between the target and current fragmentation regions and suggests more random distribution of charge in the central rapidity region. [2,6]

Weak dependence of the zone length $\langle \lambda_o \rangle$ and the zone multiplicity $\langle n_Z \rangle$ on the c.m. energy give support to the LCC hypothesis but suggest that the presently available c.m. energies are still too low for the exact energy independence of these zone parameters.

Acknowledgements

I wish to thank the members of the Fermilab-IHEP-ITEP-Michigan University collaboration and the scanning, measuring and secretarial staffs at these respective laboratories for their contribution to the experiment which has provided the data for this analysis. I am grateful to Hannu I. Miettinen, Frank Nezrick and Kenneth Lassila for useful discussions.

References

1. A. Krzywicki and D. Weingarten, Phys. Lett. 50B (1974) 265.
2. C. Bromberg et al., Physical Review D12 (1975) 1224.
3. J. Derre et al., Local compensation of charge and charge transfer in pp interactions at 69 GeV/c, A contribution to the Conference on High Energy Physics, London (1974).
4. J.P. Berge et al., Phys. Lett. 91B (1980)311.
5. P. Hoyer, Jet analysis, Lectures given at the XIX Cracow School of Theoretical Physics, Zakopane, June 1979, NORDITA preprint no. 79/33 (1979).
6. J.P. Berge et al., Quark Jets from Antineutrino Interactions I; Net charge and factorization in the quark jets, Fermilab-Pub-80/62-EXP (1980), to be published in Nuclear Physics B.
7. G. Myatt, CERN/ECFA 72-4, 11 (1972).

8. J. Blietschau et al., Phys. Lett. 87B (1979) 281.

9. D. Sinclair, Unviersity of Michigan preprint, UMBC 78-3 (1978).

10. V.V. Ammosov et al., Quark Jets from Antineutrino Interactions II; Inclusive particle spectra and multiplicities in the quark jets, to be published.

Figure Captions

Fig. 1 Illustration of the two definitions of the rapidity zones used in this analysis (shaded regions): (a) the forward c.m.s. rapidity zones for charged particles having c.m.s. rapidities $y^* > o$ (FORWARD ZONES I), and (b) the forward c.m.s. rapidity zones which include an overlapping zone (FORWARD ZONES II). The rapidity zone graph can be expressed as a sum over the final state charges, e_i, along the rapidity axis $Z(y^*) = \Sigma_i e_i \theta(y^* - y_i^*)$.

Fig. 2 Average number of rapidity zones per event as a function of average charged particle multiplicity for (a) FORWARD ZONES I and (b) FORWARD ZONES II.

Fig. 3 Length distribution of the rapidity zones, $dN_Z/d\lambda_Z$, as a function of λ_Z for FORWARD ZONES I (solid circles) and FORWARD ZONES II (solid squares). The solid lines represent exponential parameterizations of the data:

$$dN_Z/d\lambda_Z \propto \exp(-\lambda_Z/\lambda_o).$$

Fig. 4a Average length of the rapidity zones for FORWARD ZONES I (solid circles) and FORWARD ZONES II (solid squares) as functions of c.m. energy W. The open circles represent proton-proton data for central zones from Ref. 2 and 3.

Fig. 4b Average charged particle multiplicity in a rapidity zone for FORWARD ZONES I (solid circles) and FORWARD ZONES II (solid squares). The proton-proton data from Ref. 2 and 3 for central zones are shown by open circles.

Fig. 5 The average zone rapidities for FORWARD ZONES I (solid circles) and FORWARD ZONES II (solid squares) as functions of the c.m. energy.

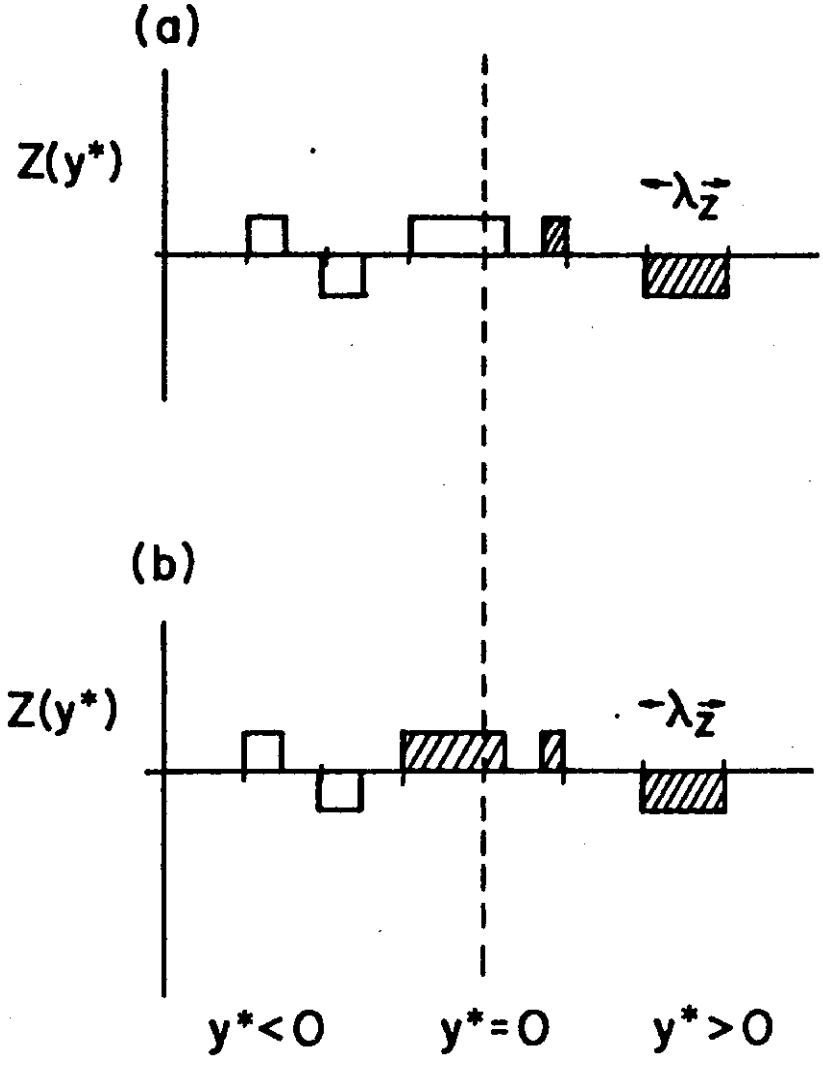

Fig. 1

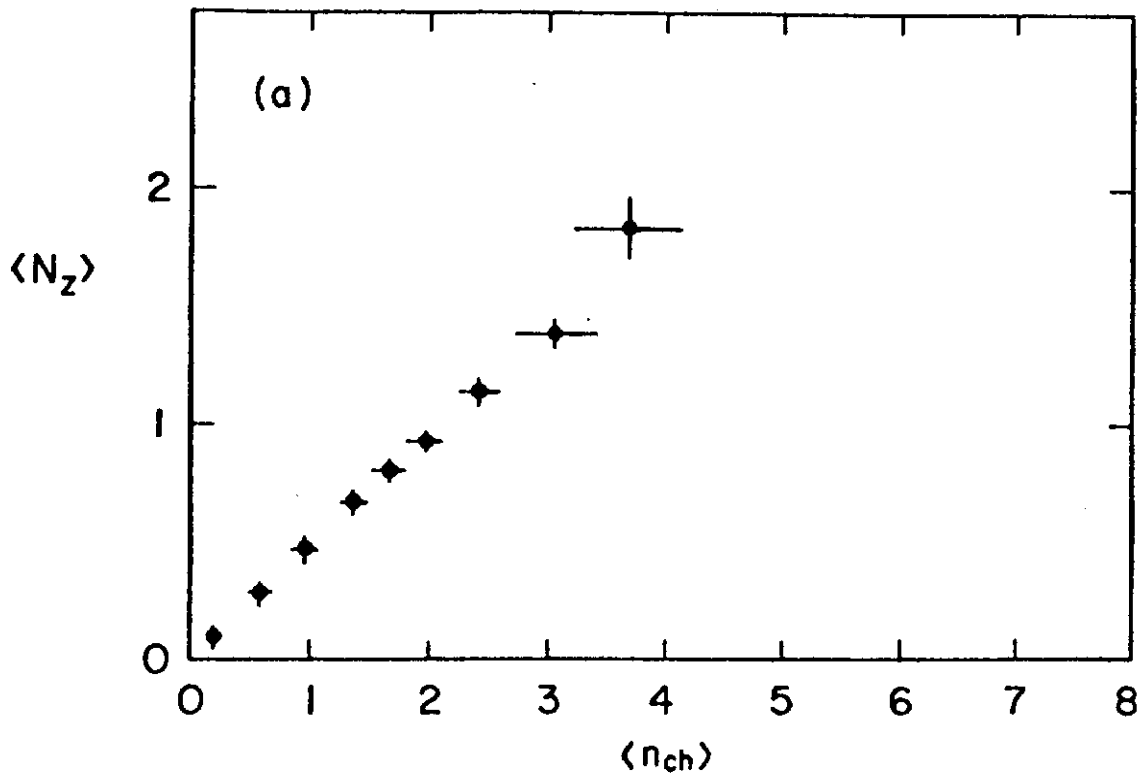
(a)
$\langle N_z \rangle$
2
1
0
0
1
2
3
4
5
6
7
8
$\langle n_{ch} \rangle$

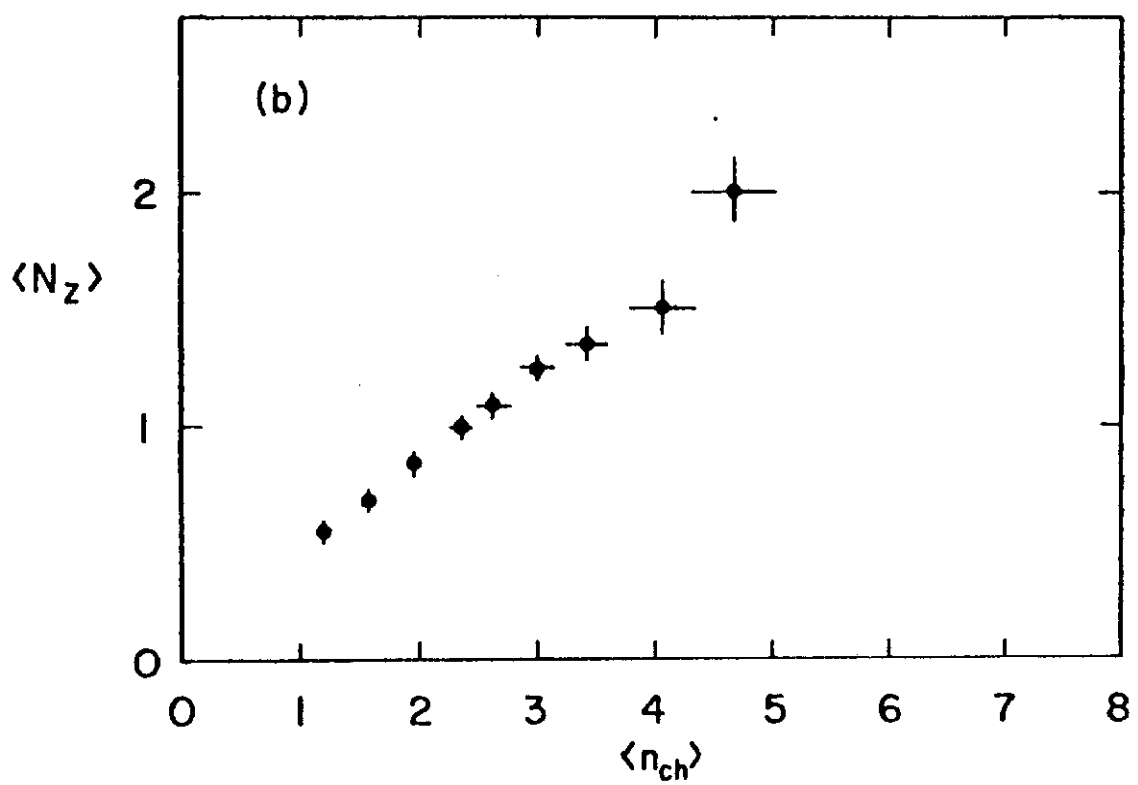
(b)
$\langle N_z \rangle$
2
1
0
0
1
2
3
4
5
6
7
8
$\langle n_{ch} \rangle$

Fig. 2

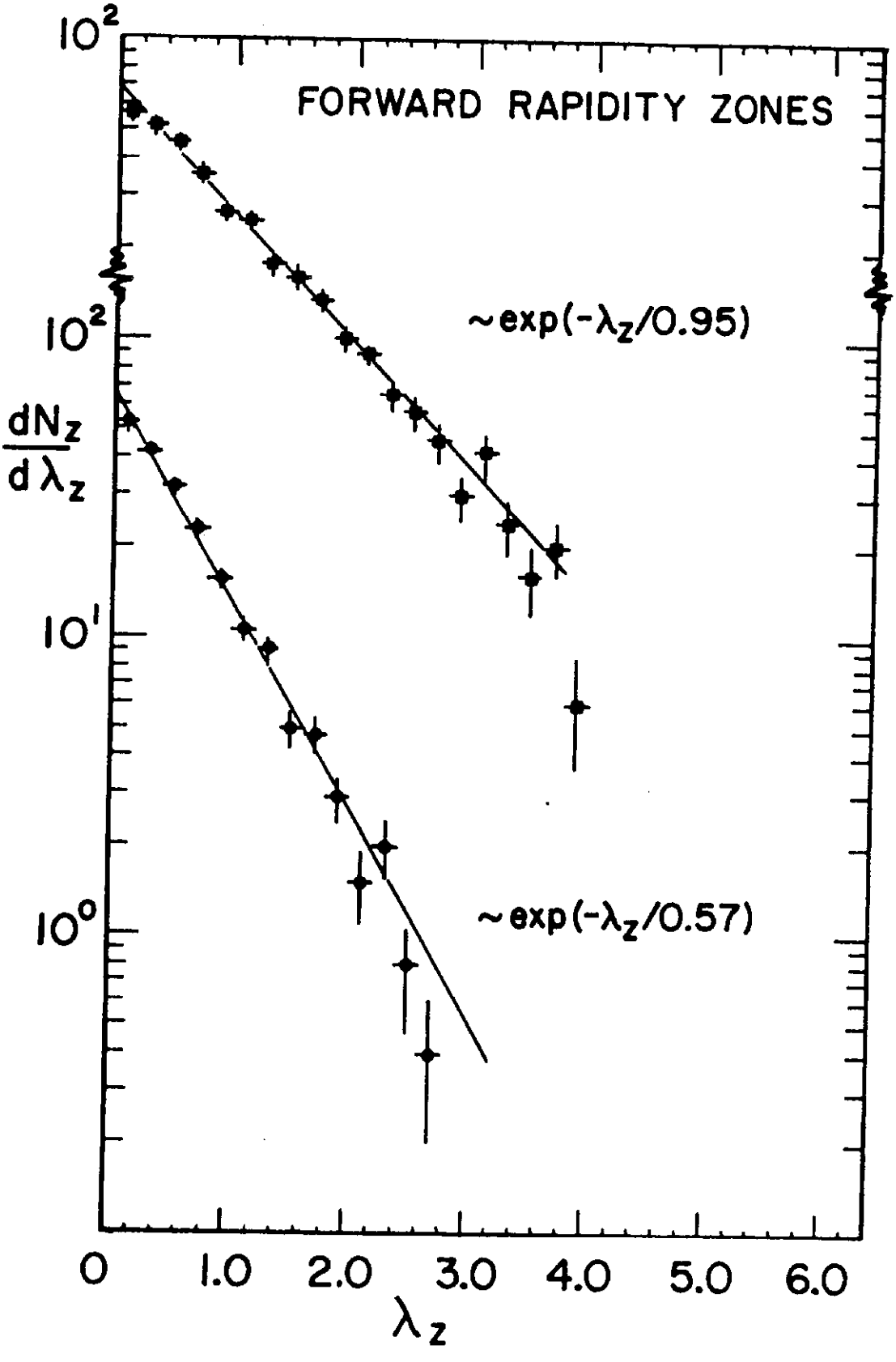
FORWARD RAPIDITY ZONES
~exp(-λz/0.95)
~exp(-λz/0.57)
dNz/dλz
λz
10²
10²
10¹
10⁰
0
1.0
2.0
3.0
4.0
5.0
6.0

Fig. 3

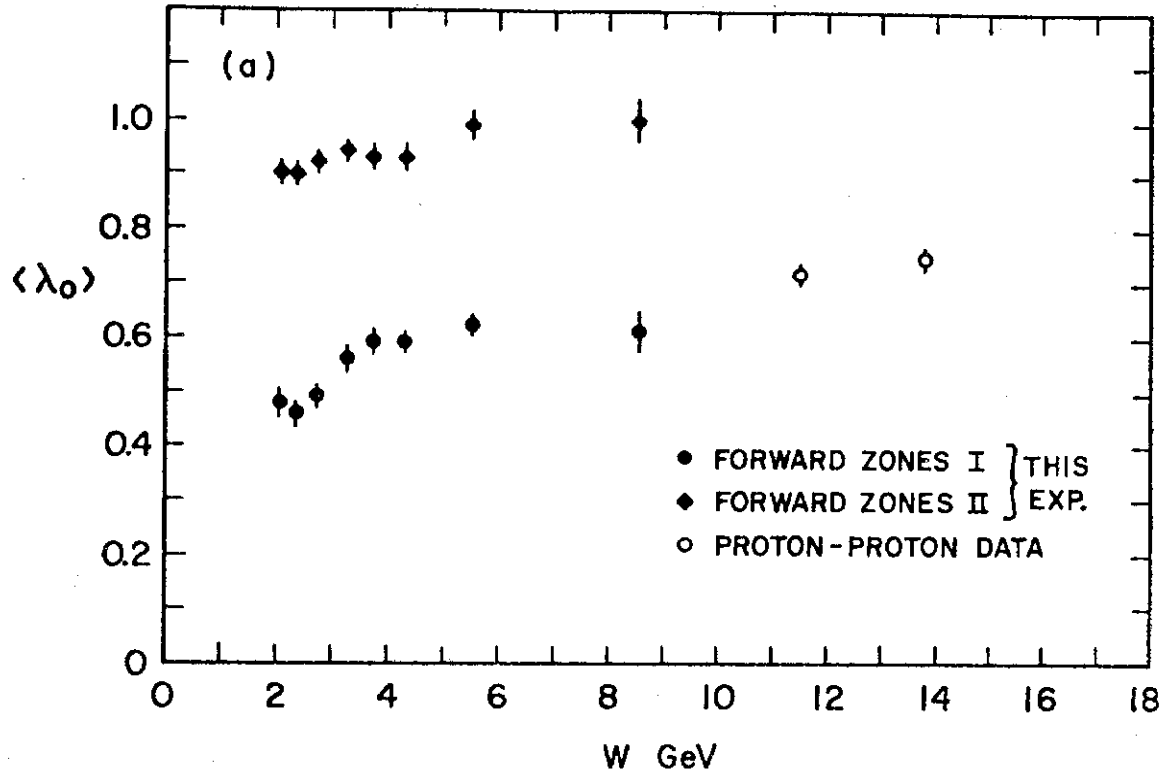
(a)
$\langle \lambda_o \rangle$
1.0
0.8
0.6
0.4
0.2
0
0
2
4
6
8
10
12
14
16
18
W GeV
FORWARD ZONES I
FORWARD ZONES II
THIS EXP.
PROTON-PROTON DATA

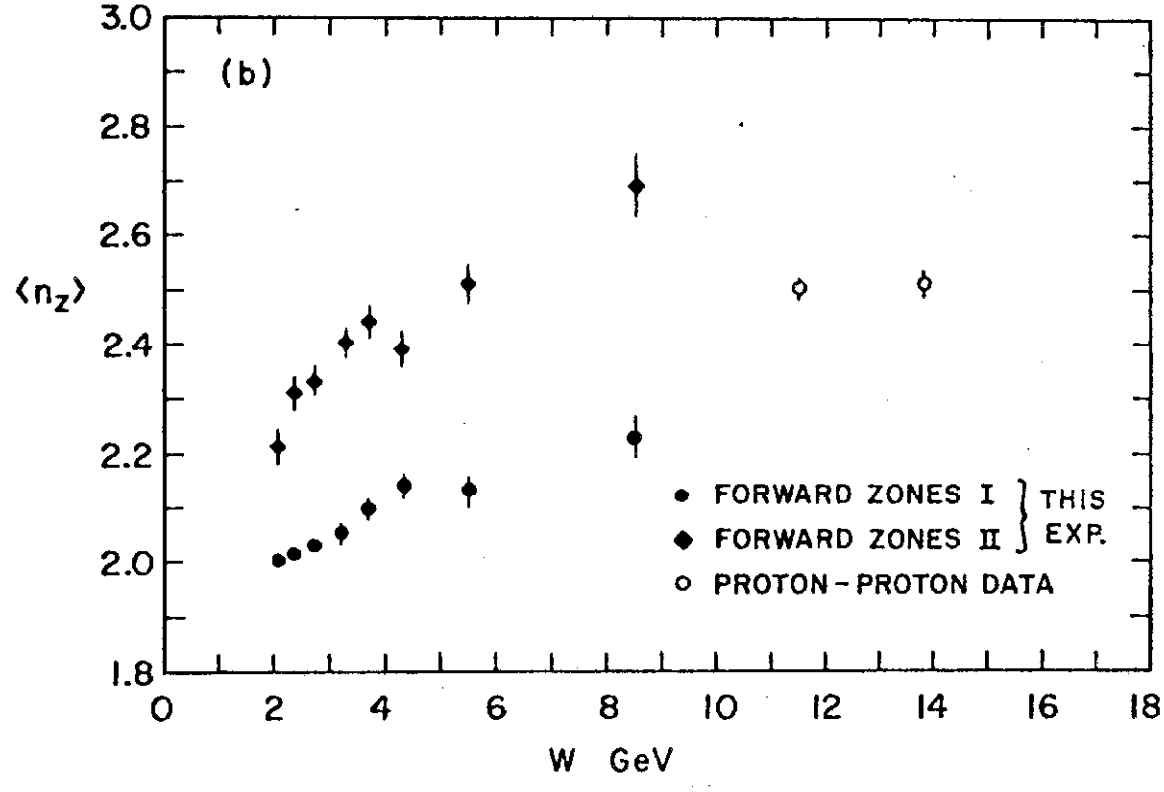
(b)
$\langle n_z \rangle$
3.0
2.8
2.6
2.4
2.2
2.0
1.8
0
2
4
6
8
10
12
14
16
18
W GeV
FORWARD ZONES I
FORWARD ZONES II
THIS EXP.
PROTON-PROTON DATA

Fig. 4

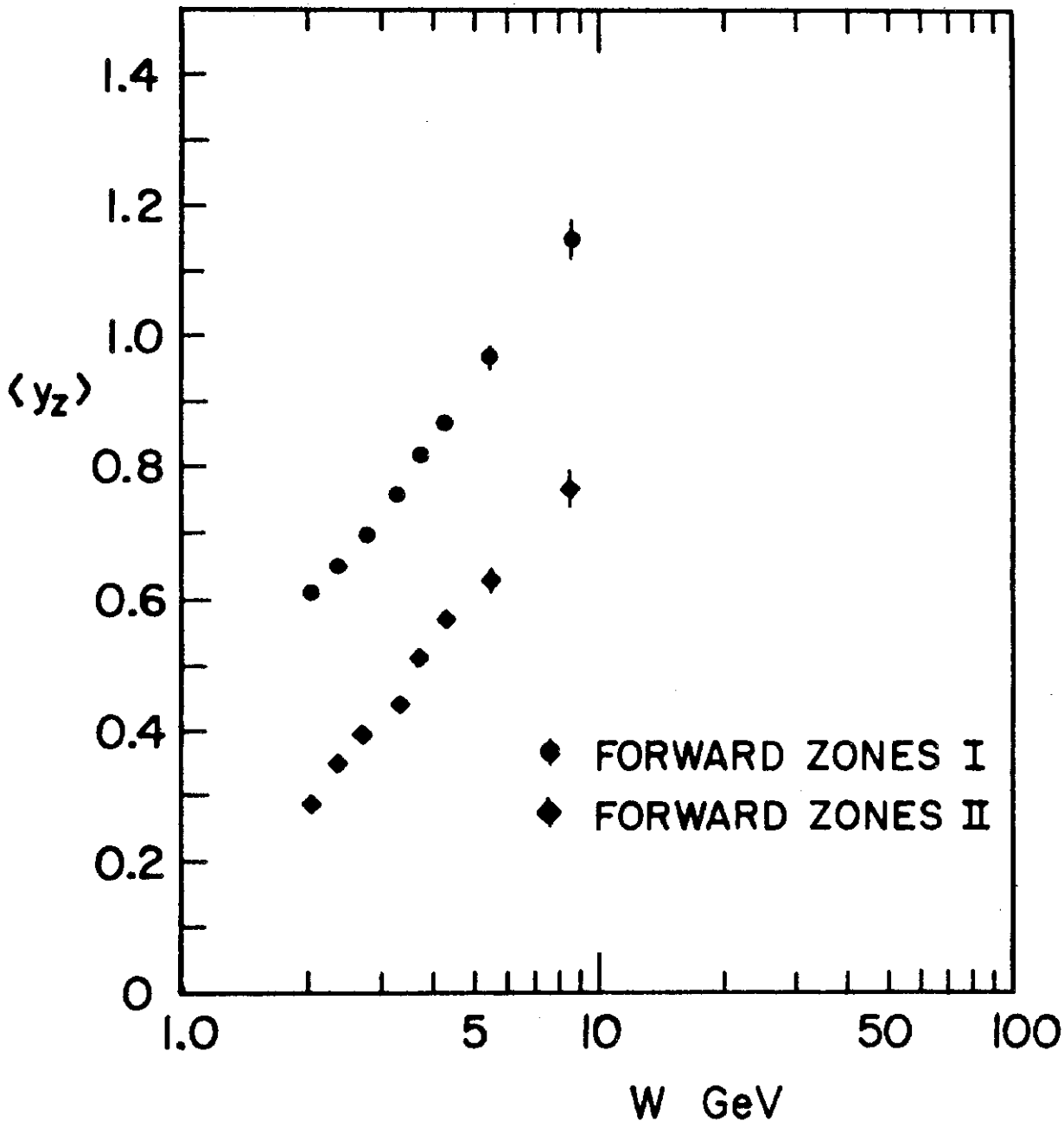
1.4
1.2
1.0
0.8
0.6
0.4
0.2
0
⟨yz⟩
1.0
5
10
50
100
W GeV
FORWARD ZONES I
FORWARD ZONES II

Fig. 5